7. Height of the boundary layer and variations above the surface layer

Tore Hattermann

Abstract

By using a helium filled balloon, to lift a thetasonde up to 900 meters height in the Adventdalen valley near to Longyearbyen, Svalbard, the boundary layer was investigated while virtual potential temperature, wind speed wind direction, relative humidity and stability is described. By launching the balloon on two different days, two different weather scenarios were found and compared, also typical regional effects were observed, finally the height of the boundary layer is determined.

7.1. Introduction

As a part of the fieldwork for the UNIS course AGF-213, Polar Metorology and climate, the height of the boundary layer will be determined and variations above the surface layer shall be described.

The boundary layer is “that part of the troposphere that is directly influenced by the presence of earths surface, and responds to surface forcings with a timescale of about an hour or less.” (Stull, 1988).

That means, while describing the boundary layer, all kind of energy exchange with surface like friction, sensible and latent heat flux or terrain inducted flow modification have to be considered. These exchanges are obviously hardly influenced by diurnal changes, due to variations of incoming solar radiation. Generally the boundary layer thickness is quite variable in time and space, ranging from hundrets of meters to a few kilometers.

To get proper vertical profiles a helium filled balloon with a theta sonde (ref. 2.5.) was launched as often as possible during the period of fieldwork at the Auroral station in the Adventdalen valley. For detailed terrain refer to waypoint 2 on the map, shown in fig. 1.1.

7.2. Theory

7.2.1. Structure of the boundary layer

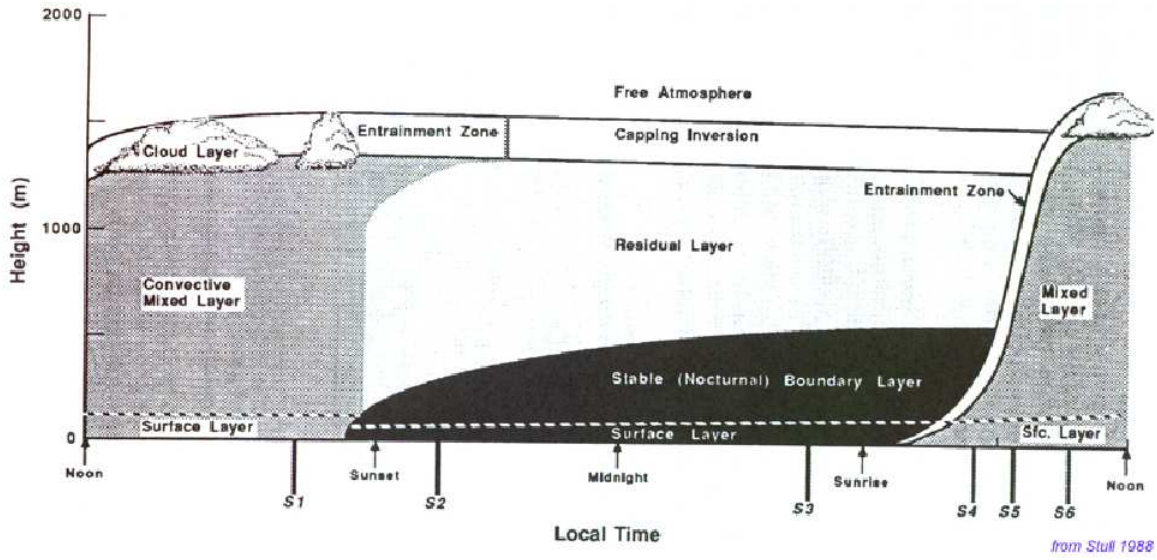

Fig. 7.1 Mayor parts of the boundary layer (From: Stull 1988)

When the boundary layer is observed above land with regular cycle of sunlight and darkness, it can be divided into four major parts:

During daytime the ground is heated by the sun and a convectively driven, vertically mixed layer grows. It reaches its maximum during the afternoon. In the mixed layer temperature decreases with height, on the bottom unstable stratification, higher up neutral stratification is observed. On top of this layer usually a stable layer acts as a lid for the rising thermals, restraining the domain of turbulence.

While heating ceases when the sun goes down, turbulence decays in the formerly mixed layer and the so called residual layer is formed. The initial mean state and concentration variables of this layer remain of the daytime mixed layer and change slowly in the absence of advection. During the night the temperature usually decreases uniform throughout the depth of the residual layer and causes neutral stratification.

Fig. 7.1 shows, that the residual layer is not in contact with the ground, therefore night processes form the stable nocturnal boundary layer. The underlying surface is colder than the air and provokes an increasing temperature with height. While the statically stable air suppresses turbulences and calms the wind speed near the surface, pressure gradients in the higher stable layer generate strong winds with wind speeds up to 10-30 m/s. The so called nocturnal or low-level jets develop wind shears that tend to generate shortly bursting turbulences. In contrast to the sharp lid which defines the top of

the mixed- and residual layer, the nocturnal boundary layer smoothly blends into the residual layer.

The surface layer is defined as 10% of the bottom of the boundary layer and has to be considered as an independent part, regardless of whether it is part of the mixed or stable boundary layer. Further more the roughness of the surface has to be taken into consideration by talking about the height of the surface layer and its conditions.

7.2.2. Concept of virtual potential temperature, stability and Richardson number

To determine the height of the boundary layer the concept of virtual potential temperature (Θ_V) is a convenient tool. It gives the temperature that dry air must have to equal the density of moist air, brought adiabatically to a certain reference pressure (p_0). It compensates for the fact, that temperature is decreasing with height due to the decreasing pressure and accounts for the changes in moisture:

$$\Theta_V = \Theta(1 + 0.61q) \qquad \textbf{(1)}$$

While

$$\Theta = T\left(p_0 / p\right)^{R/c_p} \qquad \textbf{(2)}$$

is the dry air potential temperature, calculated as an expression of pressure (p), temperature (T), R as specific gas constant and c_p as specific heat capacity of air at constant pressure. For considering the water vapor in the air, the specific humidity q has to be calculated. Therefore the relative humidity can be written as

$$\phi = \frac{q}{Q}100\% \qquad \textbf{(3)}$$

while Q is the specific humidity of saturated air at the observed temperature and pressure. It can be approximated as (ref. http://www.de.wikipedia.org, 2005)

$$Q = \frac{0.622E}{p - 0.378E} \qquad \textbf{(4)}$$

with E as the saturated water vapor pressure, calculated as

$$E = E_0 \exp\left(\frac{C_1 T}{C_2 + T}\right). \qquad \textbf{(5)}$$

Therefore we measured temperatures below zero degrees Celsius, the following constants have to be used: E_0=610.78 Pa, C_1=17.844, C_2=245.425°C. Deriving q from **(3)** and expressing Q with **(4)** and **(5)** gives the specific humidity at a certain temperature and pressure, used in **(1)**.

Therefore the vertical gradient of the virtual potential temperature gives information about the stability of stratification. For example a positive gradient means, that an upward moved air parcel due to its lower virtual potential temperature would have a lower temperature than its surrounding and drifts downwards again. Continuing this experiments of thoughts will show, that a positive vertical gradient of virtual potential temperature means stable stratification, a negative gradient means unstable stratification and a vanishing gradient means neutral stratification.

The Richardson number is used to scale the statement, which is given by the gradient of virtual potential temperature. It compares with the gravity constant g, the absolute mean temperature T_0 and the vertical wind shear of the mean wind velocity U. It is calculated as:

$$Ri = \frac{g}{T_0} \frac{\partial \Theta_V / \partial z}{\left(\partial U / \partial z\right)^2} \qquad \textbf{(2)}$$

Thus its sign is defined by the virtual potential temperature gradient, it has the same meaning but refers to a certain scale and takes the wind shear into account. Therefore the critical Richardson number Ri_{crit}=0.25 is defined as the value, which points out, whether turbulence occur or not.

7.2.3. Measurement of the boundary layer height

Usually the boundary layer shows certain profiles in virtual potential temperature, depending on time in the diurnal cycle. According to fig. 7.1, fig 7.2 shows some of these profiles at different times.

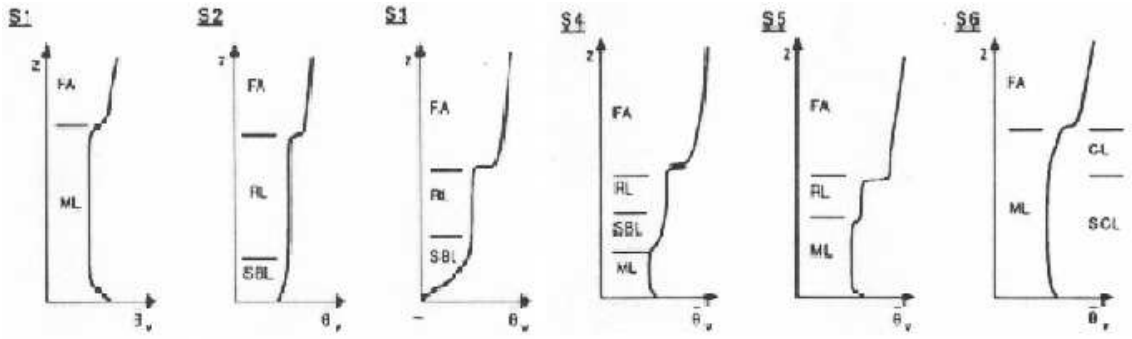

Fig. 7.2 Virtual potential temperature profiles for different snapshots of the boundary layer (From: Stull 1988)

By measuring temperature, pressure and humidity at different heights and time, the virtual potential temperature can be calcualted and its height profile will be compared with fig. 7.2., to determine its position in diurnal circle and height of the different parts of

the boundray layer. Furthermore the virtual potential temperature gradient and the Richardson number will be calculated and the results will be compared with theoretical suggestions made in section 7.1.1.. Also the wind velocity and direction will be considered to get information about the stability throughout height. With less influence from the earths surface the wind direction will turn south west, into the direction of the geostrophic wind on the northern hemisphere with increasing height.

7.3. Expectations before the field course

Since polar summer is over, diurnal changes will be observed, which is already shown in weather data from Adventdalen ground observation station.

According to steep and high mountains up to 600m, katabatic or draining winds will be observed and a high surface layer is expectable. But due to low temperatures and incoming solar radiation in general, a weaker development of the convective driven mixed layer and therefore a lower boundary layer is expectable. Also the possibility of snow cover with high albedo and less ground heating calms the effect of convective circulation and might calm the diurnal cycle in general. An inversion in the surface layer is typical for this conditions.

These contradicting effects might lead to very irregular and almost chaotic results, dominated by local systems in single valleys.

7.4. Measurements

7.4.1. Accuracy and errors

Unfortunately it is only possible to launch the balloon with low wind speed, no precipitation, so that the measurement technique already restricts the results. Further more we had to keep regulations from the aviation authorities, for not interrupting the air traffic. Due to this, the time resolution of measurements is very poor and variations with time can be hardly observed.

According to table 2.5.1, the accuracy and resolution of all parameters is acceptable compared to the scale of measured values. Only the wind speed accuracy gets in the order of ten percent of the measured wind speeds, which complicates the calculation of wind speed gradients. Another error source is the determination of the exact position of the balloon. The calculation of height by comparing pressure differences is a good approximation but due to wind drift, the balloon might move horizontally and

drive into larger turbulences instead of measuring them. Beside the length of the winch cable, this effect also restricts the maximum height of measurements.

All data is split into an up and down part, for each dataset the virtual potential temperature and its vertical gradient is calculated by formula **(1)**, smoothed with a running mean and plotted by a matlab function. Also the wind speed and direction is smoothed and plotted. Further more the Richardson number should have been calculated by formula **(2)**. But according to low and sometimes decreasing wind speeds with height, its vertical gradient which might be used for scaling is very small. This leads to unrealistic results for the Richardson number with an order of magnitude between 10^2 and 10^3.

7.4.1. Results

In total five flights, two on the 12th of September (11:10 and 12:20 UTC) and three on the 18th (9:30, 10:20 and 11:00 UTC) of September have been done (ref. table 2.5.3). The height of the flights varied between five hundred and nine hundred meters.

The following figures (fig. 7.3 till fig. 7.6) show the virtual potential temperature, its gradient and the wind speed for each flight on the 12th of September.

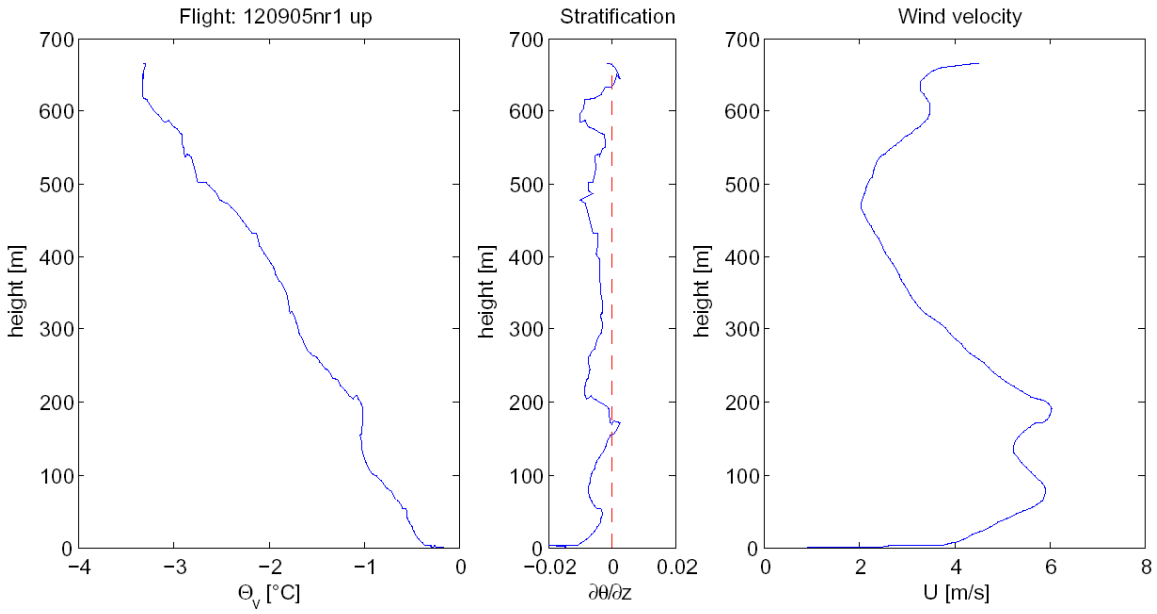

Fig. 7.3 Flight 12.09. nr. 1, 10:39-11:18 UTC, upwards, Virtual potential temperature, temperature gradient and wind speed

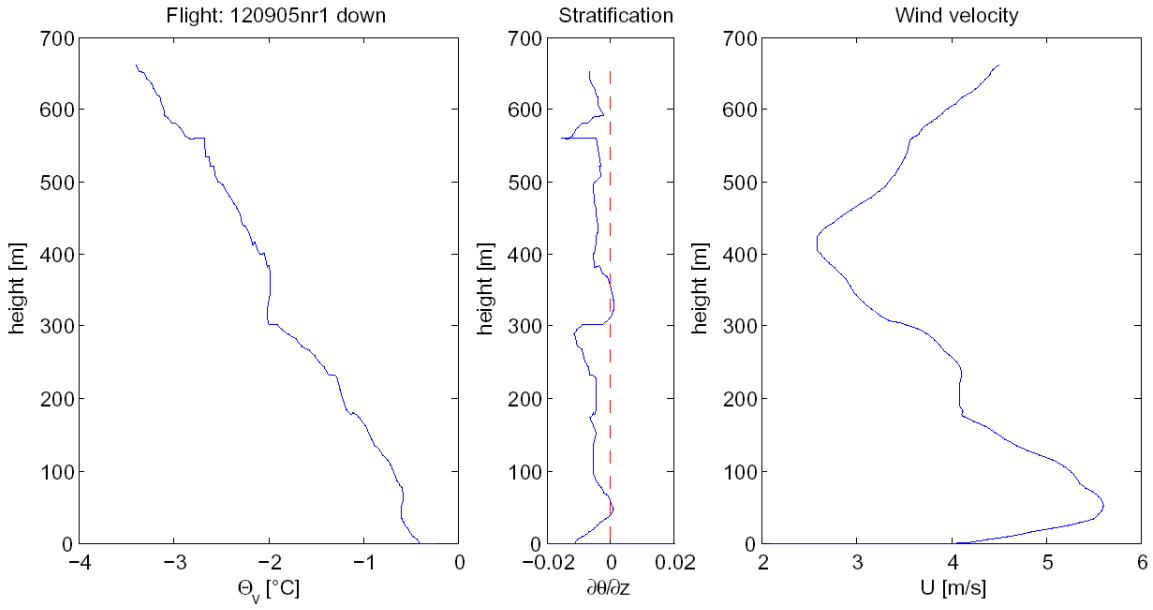

Fig. 7.4 Flight 12.09. nr. 1, 10:39-11:18 UTC, downwards, Virtual potential temperature, temperature gradient and wind speed

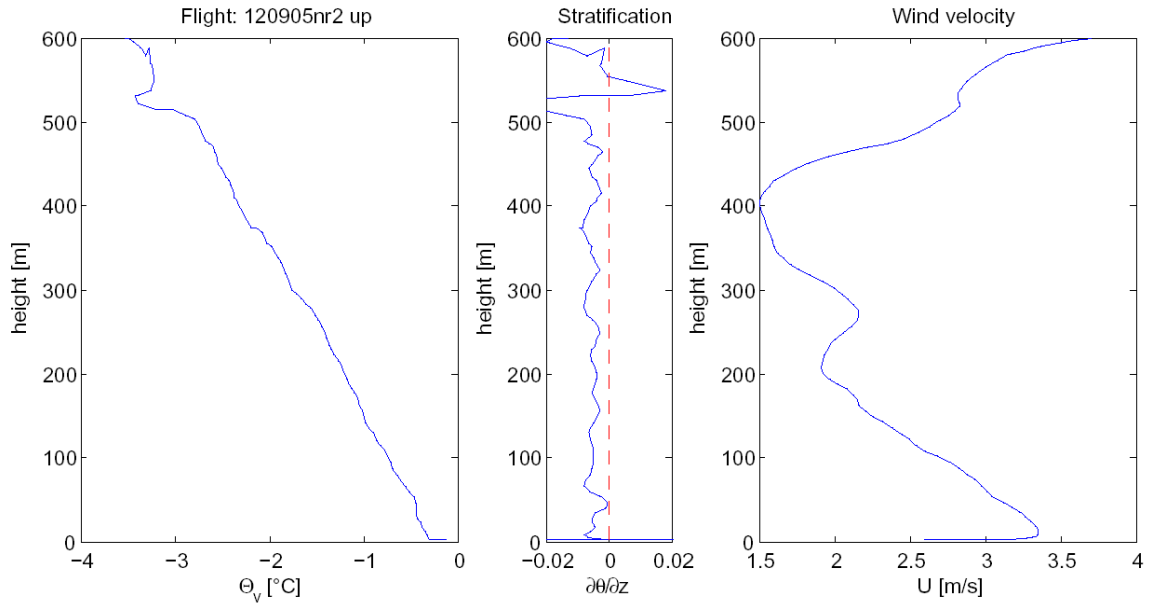

Fig. 7.5 Flight 12.09. nr. 2, 12:05-12:43 UTC, upwards, Virtual potential temperature, temperature gradient and wind speed

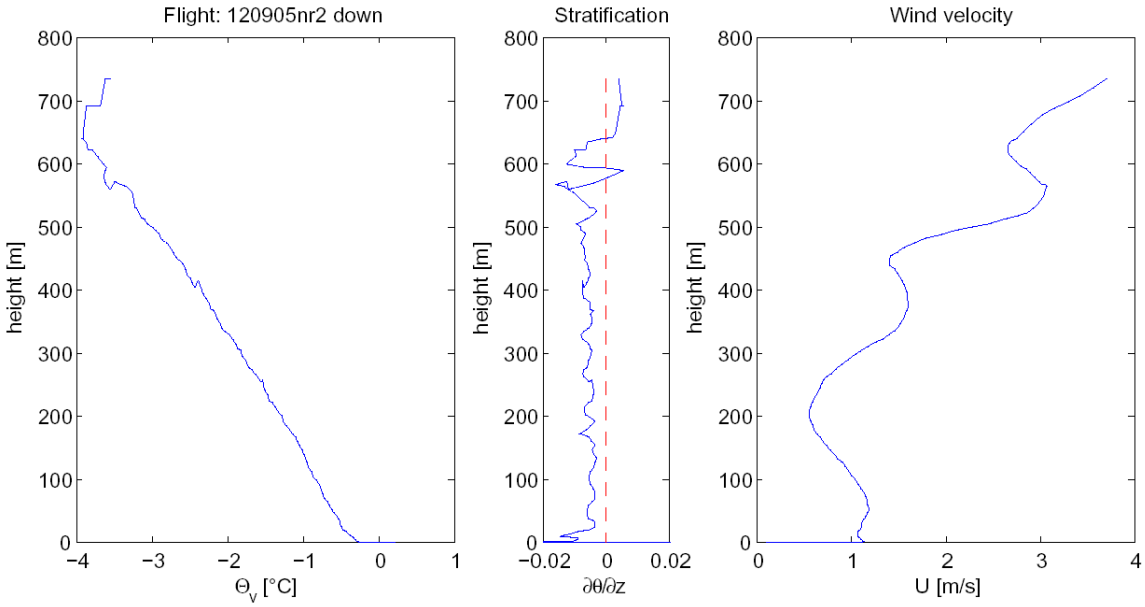

Fig. 7.6 Flight 12.09. nr. 2, 12:05-12:43 UTC, downwards, Virtual potential temperature, temperature gradient and wind speed

All flights show a dominating decrasement of virtual potential temperature with height. Fig. 7.3 also shows a small neutral or slightly inversion layer below 200 meters height, this layer seems to move upwards with time, though it can be observed in higher positions in the later flights. Furtermore an inversion or at least some irregularities can be observed in the height of 500 till 600 meters in ervery plot.

While the wind speed increases during the first hundret meters, it decreases again up to 450 till 500 meters. The following figures (fig. 7.7 and 7.8) show the wind direction of these flights. The surfcae wind direction is always almost east with round about 100 degrees, due to channeling effects in the Adventdalen valley than the winddirection varies a lot with height between 50 and 200 degrees but with a height of round about 500m the wind turns almost northernly and varies between 300 and 50 degrees. This corresponds to the wind direction, found on the analysis chart of the 12th of september, after the low pressure has passed by (refer to analysis charts fig. 2.7.4 and fig. 2.7.10).

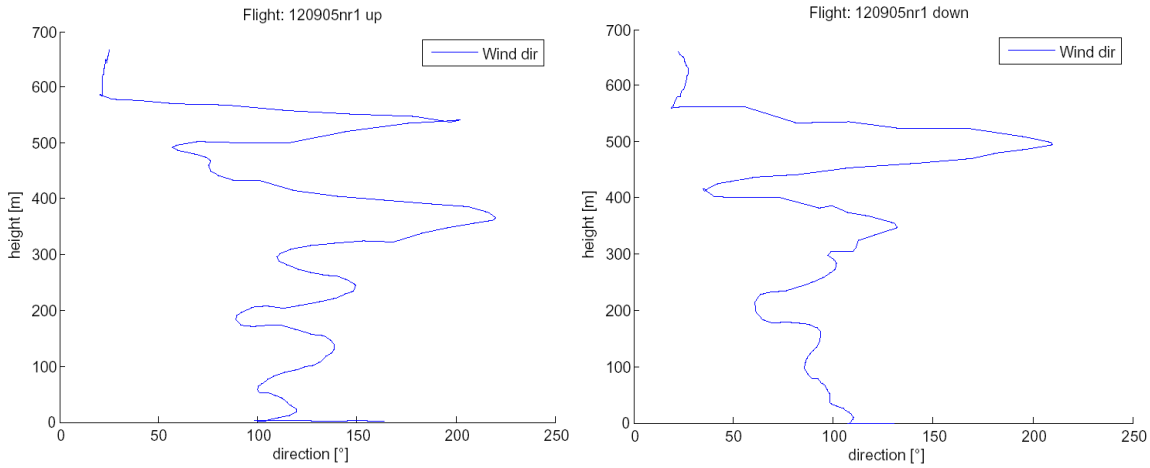

Fig. 7.7 Flight 12.09. nr. 1, 10:39-11:18 UTC, wind direction

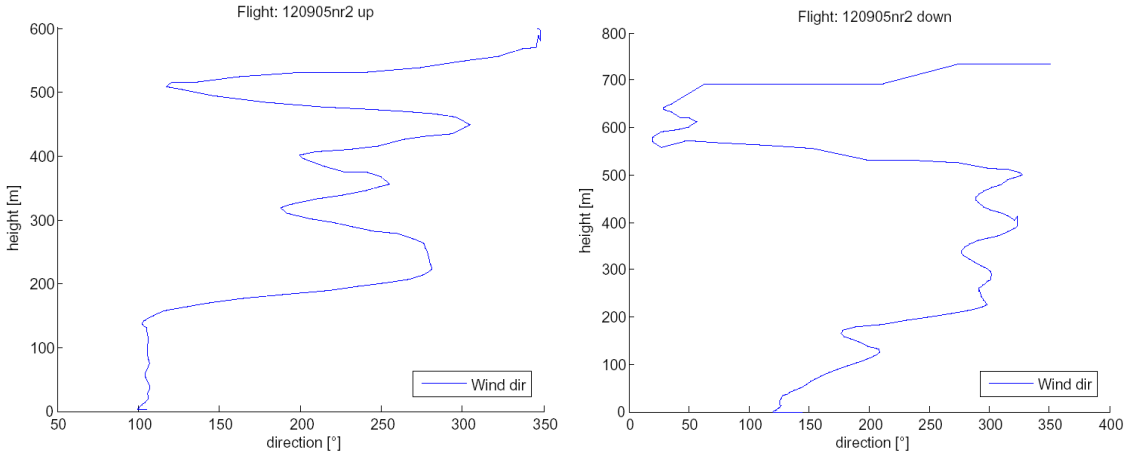

Fig. 7.8 Flight 12.09. nr. 2, 12:05-12:43 UTC, wind direction

The following figures (fig. 7.9 and 7.10) show the relative humidity profiles of these flights. The relative humidity is mainly increasing throughout height, and therefore an inverse behavior, compared to the temperature profile is observed. This is reasonable, cold air can keep less water vapor than warm air. Also the irregularities observed in temperature and wind speed and direction can be observed. Even the small, upwards moving layer below 200 meters during the first flight seems to point out with an irregular high relative humidity.

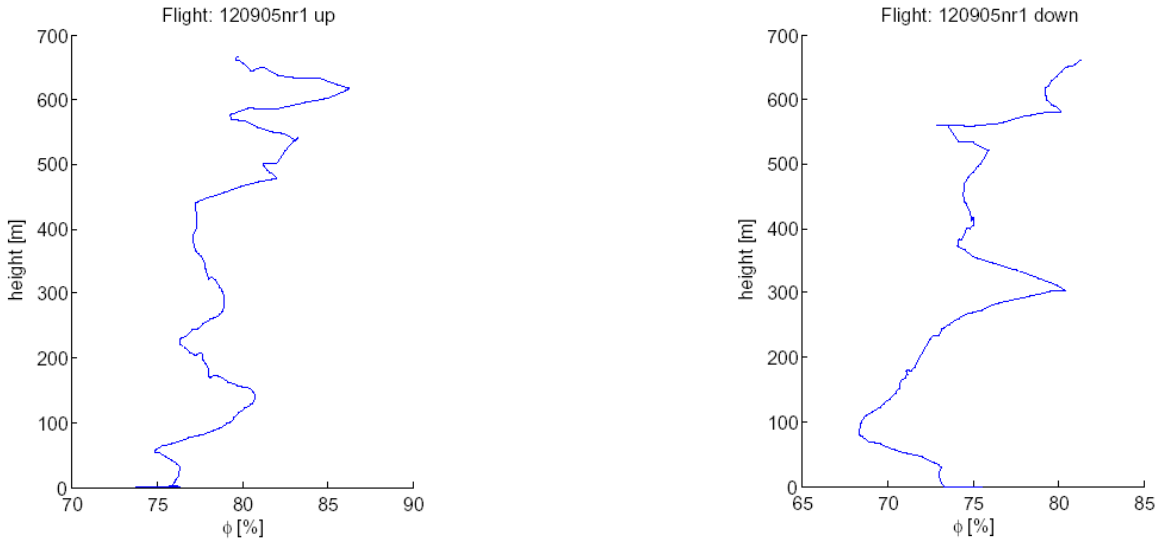

Fig. 7.9 Flight 12.09. nr. 1, 10:39-11:18 UTC, relative humidity

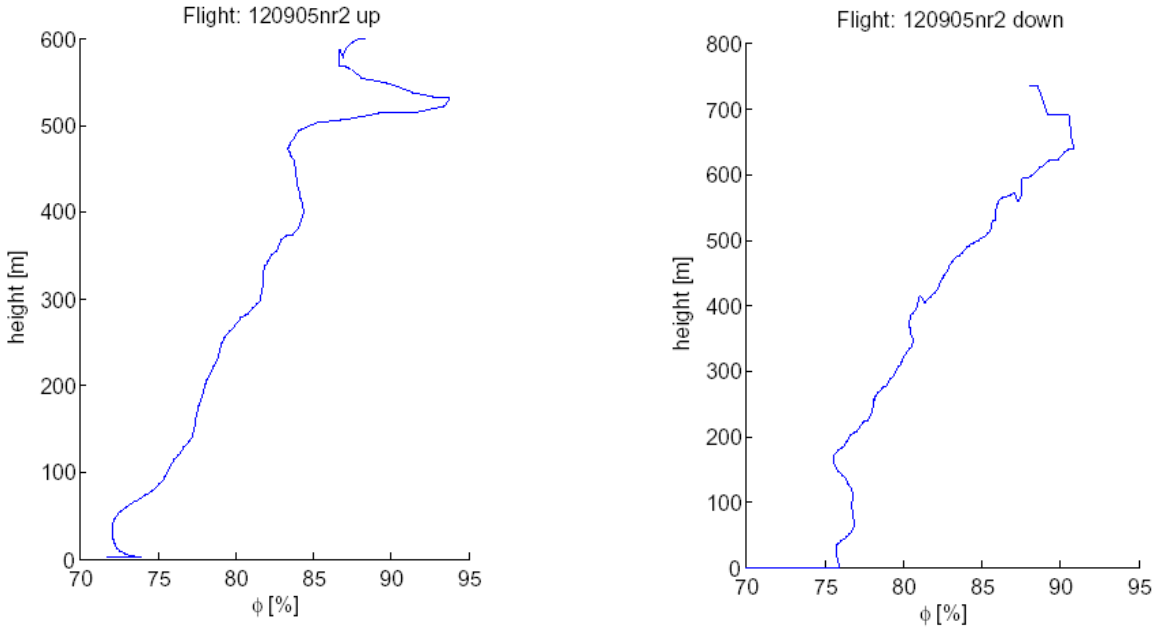

Fig. 7.10 Flight 12.09. nr. 2, 12:05-12:43 UTC, relative humidity

The inversion layer at 500 till 600 meters height, the increasing wind speed and the change in wind direction and relative humidity might point out the top of the convective mixed layer, which should be developed at the measuring time, corresponding to fig. 7.2. Therefore this inversion layer might be the top of the boundary layer. Compared to the internal layer which was pointed out to move upwards, this toplayer seems to be constant in height.

The following figures (fig. 7.11 till fig. 7.14) show the virtual potential temperature, its gradient and the wind velocity for the first and third flight on the 18th of September. The 2nd flight which was taken level by level is not that good for high resoluted profile plots and is therefore neglected.

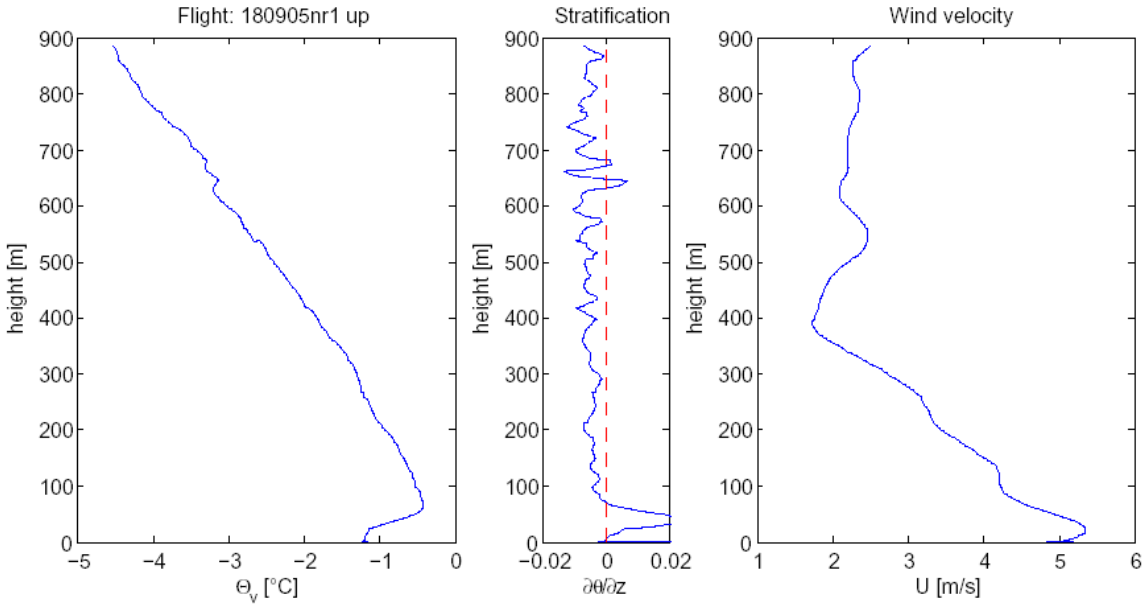

Fig. 7.11 Flight 18.09. nr. 1, 08:37-09:27 UTC, upwards, Virtual potential temperature, temperature gradient and wind speed

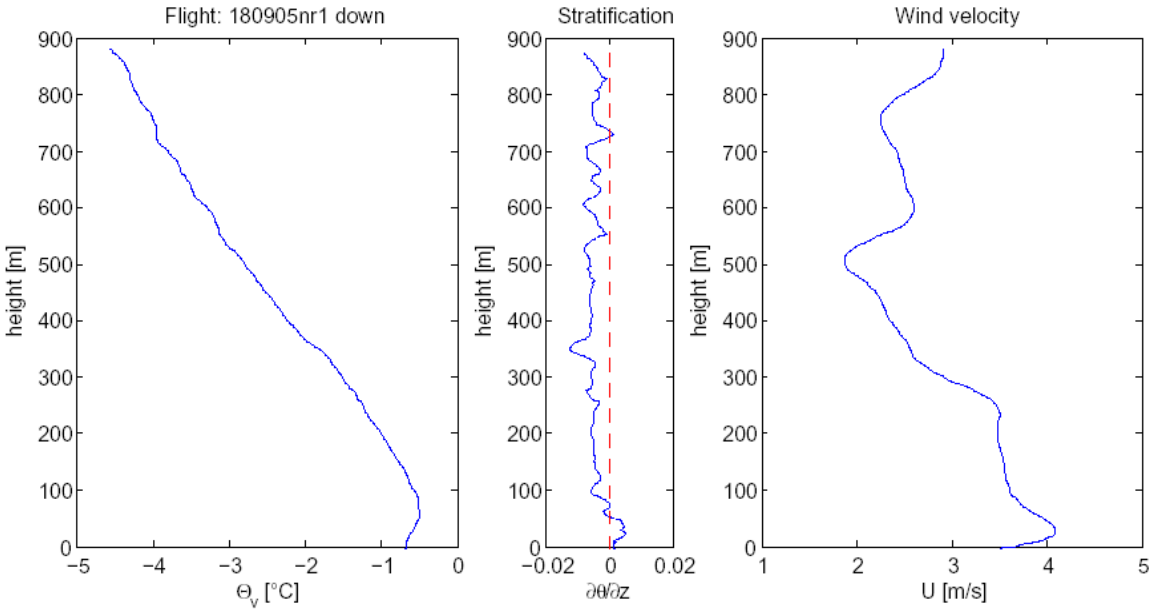

Fig. 7.12 Flight 18.09. nr. 1, 08:37-09:27 UTC, downwards, Virtual potential temperature, temperature gradient and wind speed

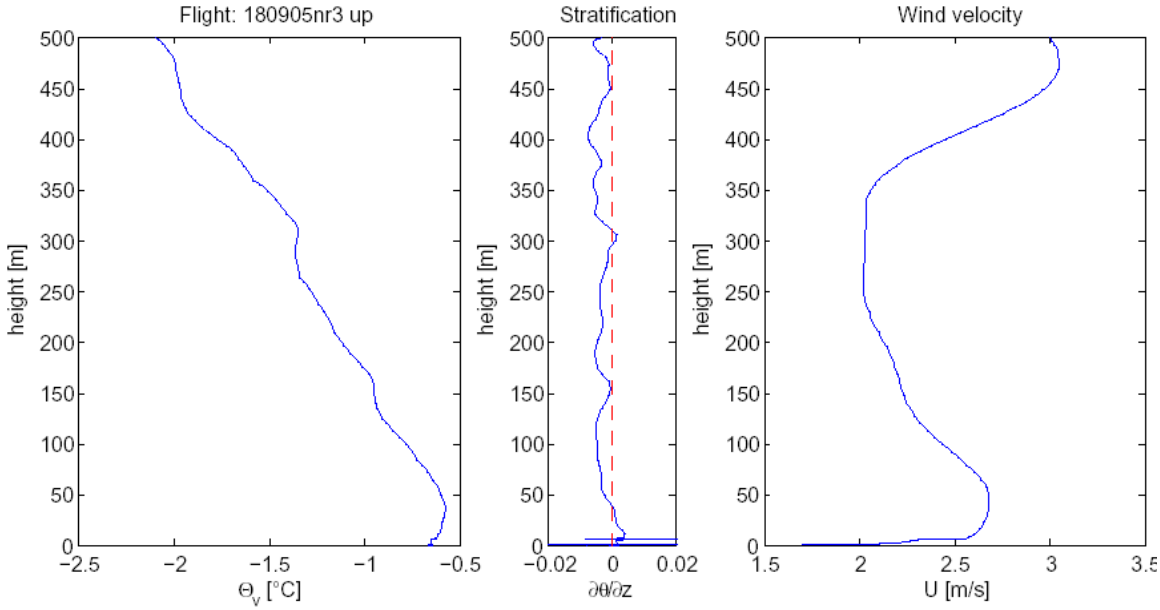

Fig. 7.13 Flight 18.09. nr. 3, 10:25-10:56 UTC, upwards, Virtual potential temperature, temperature gradient and wind speed

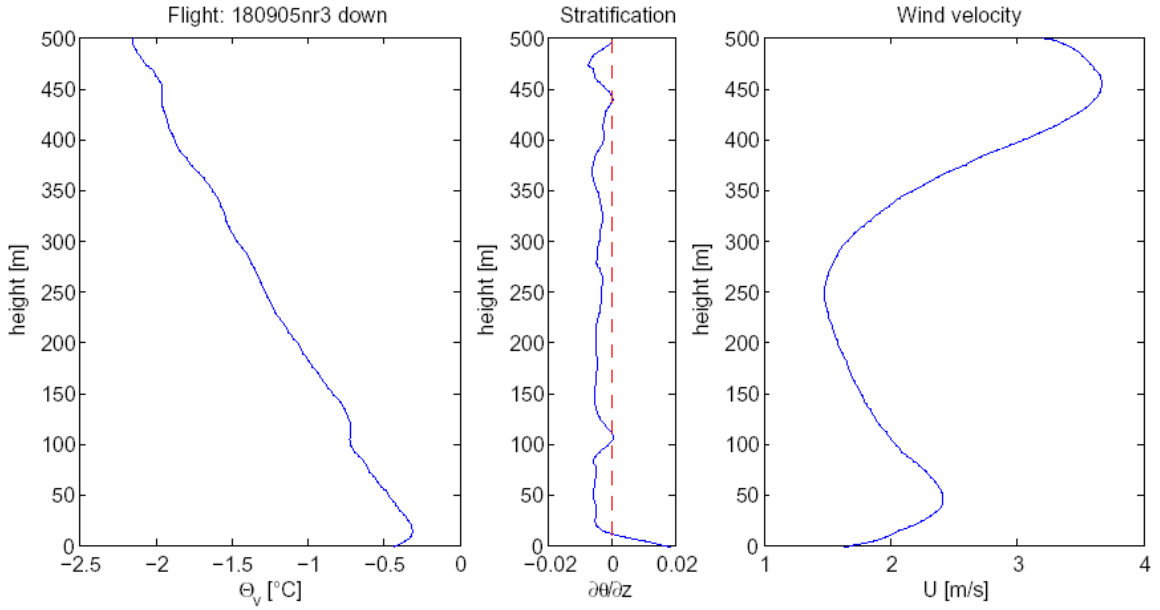

Fig. 7.14 Flight 18.09. nr. 3, 10:25-10:56 UTC, downwards, Virtual potential temperature, temperature gradient and wind speed

All profiles show a definitive stable inverse layer during the first 50 till 100 meters, which is typical for arctic, snow covered regions. Then the virtual potential temperature decreases with height and a small inversion layer is observed in the height of 600 and 700 meters at least during the first flight. The third flight was only taken up to 500 meters and shows also some inversions or at least neutral conditions in the height of 100 till 150 meters, 300 meters and 400 meters which seem to be various internal layers.

The following figures (fig. 7.15 and 7.17) show the wind direction of all flights on the 18th of September. Although all plots show a lot variations in their specific profile they have in common, that the wind direction at the surface points out east, south east around 100 and 150 degrees and turns throughout height via south till south west around 200 till 240 degrees, which is the direction of geostrophic wind.

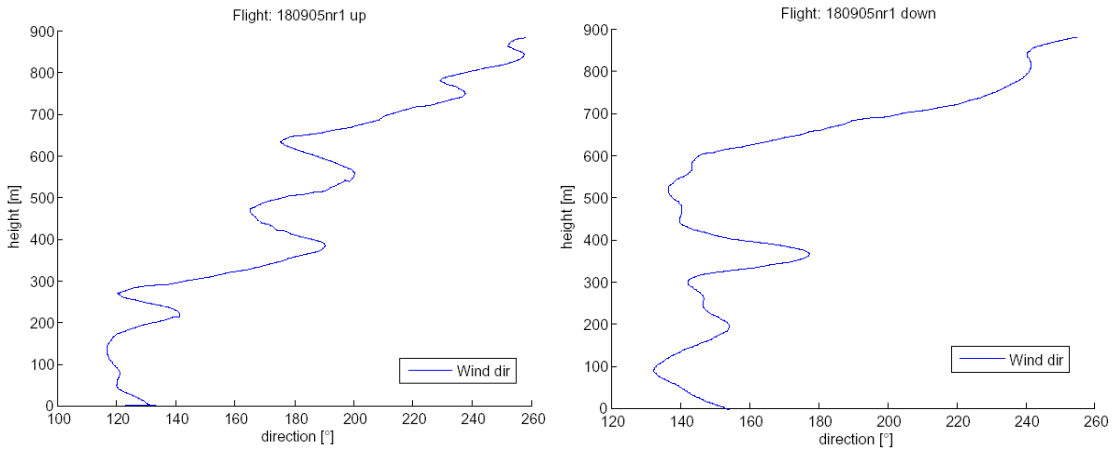

Fig. 7.15 Flight 18.09. nr. 1, 10:39-11:18 UTC, wind direction

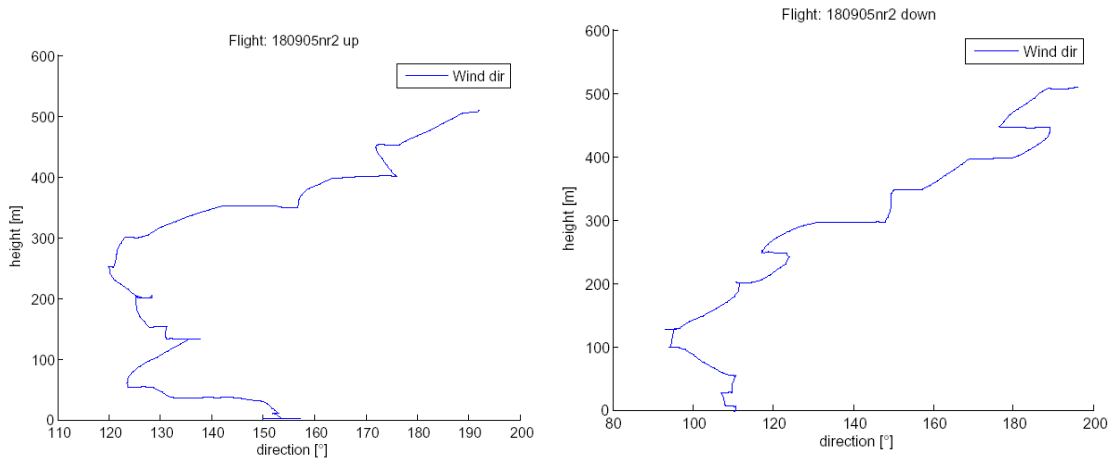

Fig. 7.16 Flight 18.09. nr. 2, 12.05-12:43 UTC, wind direction

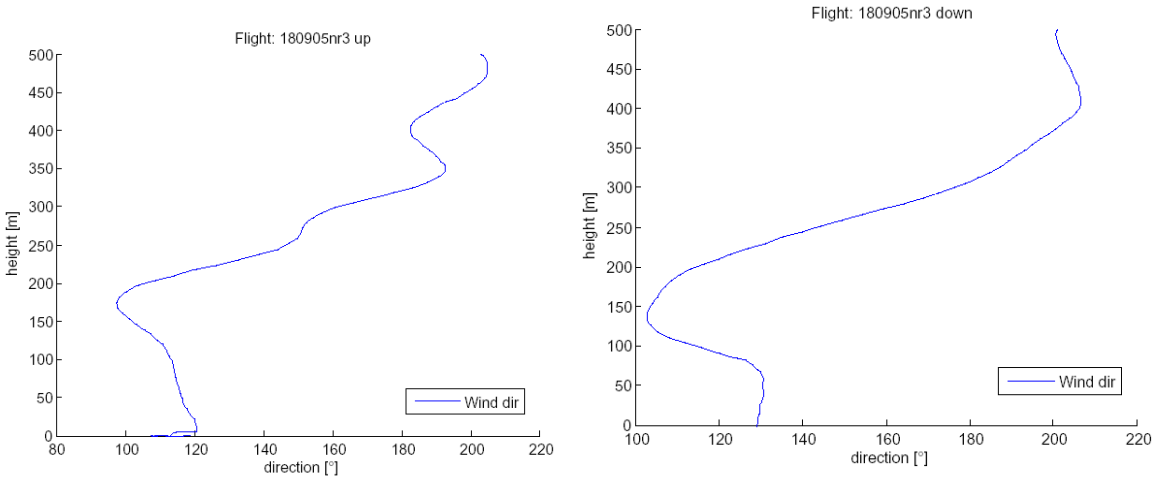

Fig. 7.17 Flight 18.09. nr. 3, 10:25-10:56 UTC, wind direction

The following figures (fig. 7.18 and 7.20) show the relative humidity profiles of all flights of the 18th of September. Also the mentioned irregularities in temperature occur and confirm the assumptions above.

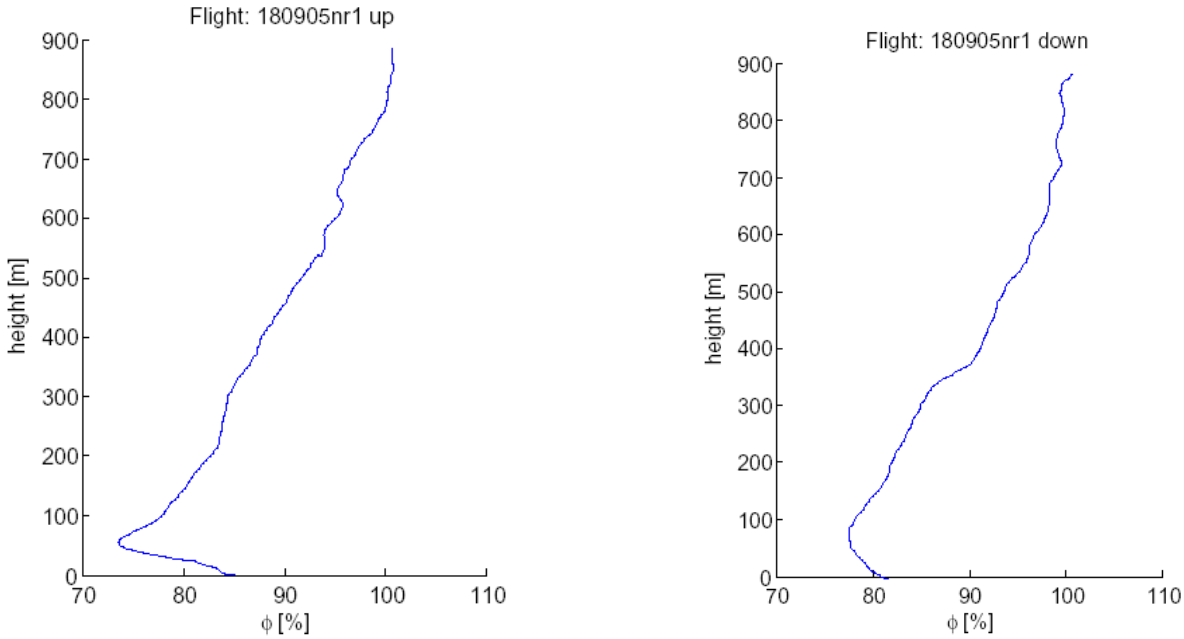

Fig. 7.18 Flight 18.09. nr. 1, 10:39-11:18 UTC, relative humidity

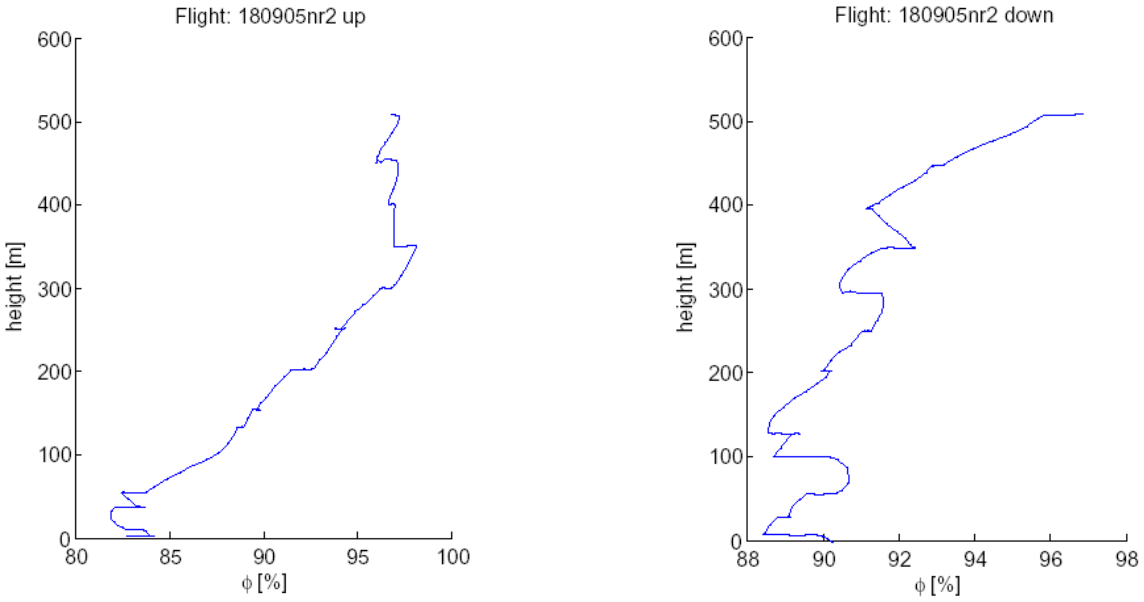

Fig. 7.19 Flight 18.09. nr. 2, 12.05-12:43 UTC, relative humidity

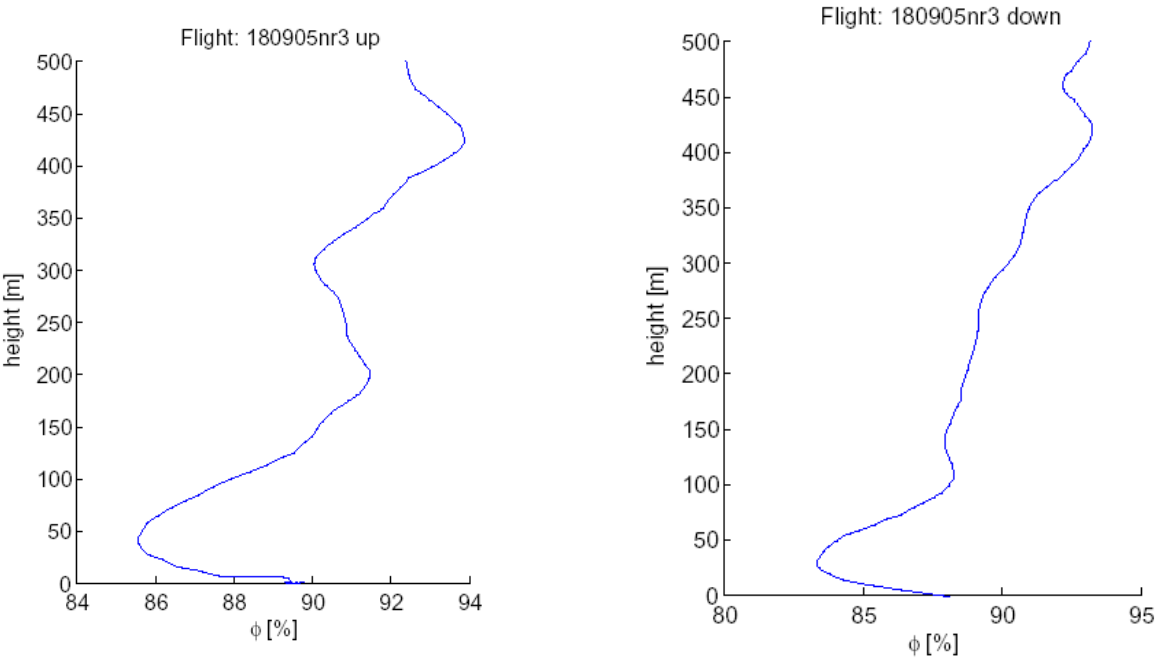

Fig. 7.20 Flight 18.09. nr. 3, 10:25-10:56 UTC, relative humidity

On this day it is much more difficult to identify a certain height, which determines the boundary layer height. Anyway the situation is completely different from the results on the 12th of September. Probably that day was directly influenced by the strong low pressure zone, passing by. In that situation the surface influenced boundary layer might have been lower than on the calm day of 18th of September where, corresponding to the analysis charts no fronts and wide isobars were observed. In this case the height where the wind turns in geostrophic direction determines the top of the boundary layer, which

would be between 700 and 800 meters, this also corresponds to the small inversion, observed between 600 and 700 meters.

7.5. Conclusion

Both measurement periods have been taken place during the late morning and noon time though a developed convective mixed layer is expectable, this seems to be validated by slightly unstable stratification almost through the whole profile. Also wind channeling near to the ground, caused by the Adventdalen valley shows up in all profiles.

Nevertheless the measurements show two completely different weather situations. On the 12th of September, the boundary layer was definitely influenced by the active larger scale weather scenario and on the 18th of September a rather typical calm situation with its typical phenomena like a stable stratified surface layer due to snow cover and turning wind direction into the direction of geostrophic wind was observed.

The absolute height of the boundary layer might also be determined and lies between 500 and 600 meters on the 12th of September and between 700 and 800 meters on the 18th of September. But though the balloon was not launched much higher than these results they are quite uncertain.

Due to less flights a time resoluted variation of the boundary layer height can not be given.

1.5. References

Stull R., 1988, An Introduction to Boundary Layer Meteorology, Kluwer Academic Publishers

Sjöblom A., 2005, AGF-213 lecture Notes, UNIS

http://de.wikipedia.org/wiki/Magnus_Formel, 20-10-2005, 15:00